Screen-printed electrodes modified with carbon nanotubes or graphene for simultaneous determination of melatonin and serotonin

Federico José Vicente Gomez, Aída Martín, María Fernanda Silva & Alberto Escarpa

Microchimica Acta
Analytical Sciences Based on Micro- and Nanomaterials

ISSN 0026-3672

Microchim Acta
DOI 10.1007/s00604-015-1520-x

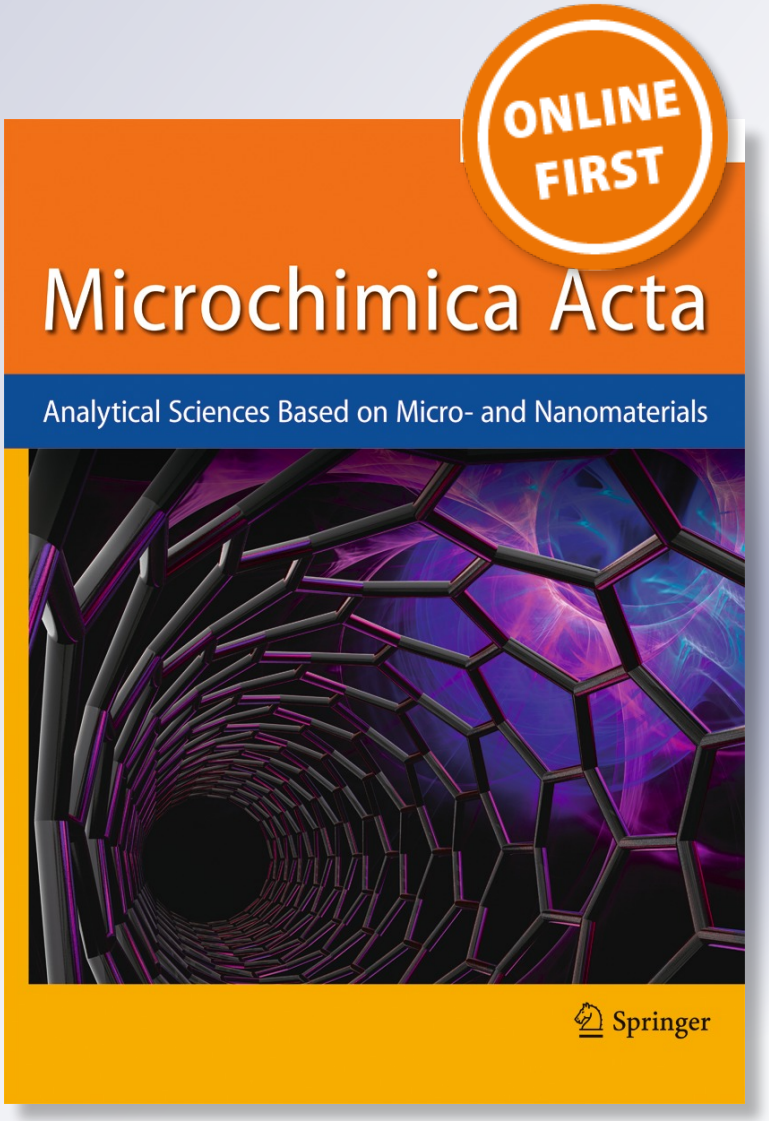

Springer

Microchim Acta
DOI 10.1007/s00604-015-1520-x

ORIGINAL PAPER

Screen-printed electrodes modified with carbon nanotubes or graphene for simultaneous determination of melatonin and serotonin

Federico José Vicente Gomez[1,2] · Aída Martín[1] · María Fernanda Silva[2] · Alberto Escarpa[1]

Received: 20 March 2015 / Accepted: 8 May 2015

Abstract Single-walled carbon nanotubes (SWCNT), multi-walled carbon nanotubes (MWCNT) and graphene have been tested as carbon allotropes for the modification of carbon screen-printed electrodes (CSPEs) to simultaneously determine melatonin (MT) and serotonin (5-HT). Two groups of CSPEs, both 4 mm in diameter, were explored: The first includes commercial SWCNT, MWCNT and graphene, the second includes SWCNT, MWCNT, graphene oxide nanoribbons and reduced nanoribbons that were drop casted on the electrodes. The carbon nanomaterials enhanced the electroactive area in the following order: CSPE <MWCNTs <SWCNTs <graphene. This allowed the simultaneous determination of 5-HT and MT at the working potentials of + 50 mV and +390 mV (vs. Ag), respectively. The use of carbon nanomaterials, in particular of graphene oxide nanoribbons on CSPEs, represents an excellent and disposable tool for sensing the two target molecules in even small sample volumes. Figures of merit for MT and 5-HT include (a) detection limit of 1.1 and 0.4 μM for MT and 5-HT, respectively; (b) an inter-electrode reproducibility with RSD ≤ 8 %; (c) 120 s response time, and (d) recoveries (in case of spiked samples) ranging from 94 to 103 % (with an RSD < 1 %).

✉ Alberto Escarpa
alberto.escarpa@uah.es

[1] Department of Analytical Chemistry, Physical Chemistry and Chemical Engineering, Faculty of Chemistry, University of Alcalá, 28871 Alcalá de Henares, Madrid, Spain

[2] Instituto de Biología Agrícola de Mendoza (IBAM-CONICET), Facultad de Ciencias Agrarias, Universidad Nacional de Cuyo, 5505 Mendoza, Argentina

Keywords Screen-printed electrode · Carbon nanomaterials · Single and multi-walled carbon nanotubes · Graphene · Graphene nanoribbons · Melatonin · Serotonin

Introduction

Carbon nanomaterials such as carbon nanotubes (CNTs) and graphene have been widely used in electroanalysis. Their high surface areas and electrical conductivities are quite attractive features in terms of electrochemical sensing and biosensing [1, 2]. The large surface area of these carbon nanomaterial-based electrodes allows detection potentials to be decreased (thus improving the selectivity of analysis), while amperometric faradic currents are increased (leading to enhanced analytical sensitivity) and surface fouling is reduced (thereby improving reproducibility) [2–4].

On the other hand, screen-printing technology represents a well-established technique for the fabrication of electrochemical sensors with high sensitivity and selectivity, with all the benefits of an easily renewable sensor. In particular, the possibility to regularly change the sensor allows reducing the risk of contamination from one analysis to another. In addition, the incorporation of carbon nanostructures such as carbon nanotubes first, and more recently graphene, have considerably changed the scope of carbon-based electrodes in electroanalysis [3]. Furthermore, there are a large number of commercially available electrodes, modified with nanomaterials, which constitute another valuable feature of this technology.

Hence, carbon nanomaterial-based sensors on screen-printed platforms constitute useful tools for (rapid and cheap) analysis and screening. Here, we have explored a set of carbon nanomaterial-based screen-printed electrodes for the detection

Published online: 26 May 2015

of two significant target electroactive molecules, melatonin (MT) and serotonin (5-HT), which chemical structures are shown in Fig. 1.

MT (N-acetyl-5-methoxytryptamine), known as the molecule of darkness, is a multifunctional indoleamine synthesized from L-tryptophan metabolism via serotonin. It was exclusively considered an animal hormone, specifically a neurohormone, for nearly four decades until its discovery in plants. Since then, it has been found in more than 140 different plant species and foods [5–13]. Furthermore, healthy subjects synthesize melatonin not only in the pineal gland [14], but also in a wide range of other organs.

5-HT (5-hydroxytryptamine, serotonin) is an important monoamine neurotransmitter widely dispersed throughout the central nervous system, which plays a crucial role in the regulation of mood, sleep, and appetite. It has also been reported that foods and plants contain significant quantities of serotonin [15, 16]. MT usually appears in the presence of 5-HT; therefore, their simultaneous determination may be extremely important to understand biological systems and samples.

Several analytical techniques have been developed for the simultaneous measurement of 5-HT and MT, liquid chromatography coupled to mass spectrometry and capillary electrophoresis with UV detection being most often used [16–19]. Although these methods can adequately monitor the levels of 5-HT and MT, they still require skilled personnel and sophisticated and expensive instrumentation. In contrast, electrochemical techniques possess analytical and economic advantages including simple instrumentation and low-cost, high sensitivity, fast response and easy operation. In this way, it is important to point out that MT has not extensively been studied using electroanalytical approaches [20–24] and rarely the simultaneous detection of both 5-HT and MT molecules has been explored [21]. This relevant bibliography is also supported by recent reviews which have shown the significance of the nanomaterial-based approaches for electrochemical sensing of biogenic amines [25] and neurological drugs and neurotransmitters [26]. However, the exploration of the important combination of the target technologies –screen-printing and nanotechnologies– in electroanalytical chemistry has not been studied in detail for the simultaneous detection of these significant molecules.

Therefore, here, we investigate the use of carbon nanomaterial-based screen-printed electrodes for the simultaneous detection of 5-HT and MT. To this end, a set of carbon nanomaterial-based screen printed electrodes (commercially available and in-lab modified electrodes) will be critically evaluated.

Materials and methods

Chemicals

MT and 5-HT were purchased from Sigma Chemical (St. Louis, MO, USA). Sodium hydrogen phosphate and sodium dihydrogen phosphate were purchased from Panreac, (Badalona, Spain). Phosphate buffer 5 mM was prepared by dissolving appropriate amounts of sodium hydrogen phosphate and sodium dihydrogen phosphate. The solution pH was adjusted to 7.6 by addition of 1 M sodium hydroxide solution. Ultrapure water (18 MΩ cm) was obtained from Milli-Q system (Millipore, Bedford, MA, USA).

Apparatus

All electrochemical measurements were performed, at room temperature, on an USB-based portable electrochemical station μ-Stat 100 potentiostat controlled by PSLite 1.6 software, by a carbon screen-printed electrode (CSPE), which integrates a three-electrode system based on carbon as counter electrode, working electrodes of 4 mm diameter and a silver reference electrode (Dropsens, Oviedo, Spain).

Electrodes and carbon materials

Two groups of carbon electrodes were explored: commercial and modified electrodes. Commercial screen-printed electrodes, which were purchased from DropSens (http://www.dropsens.com) (Oviedo, Spain) including carbon ink (DRPC100), MWCNTs ink (DRP-110CNT), SWCNTs ink (DRP-SWCNT), and graphene ink (DRP-110GPH). The

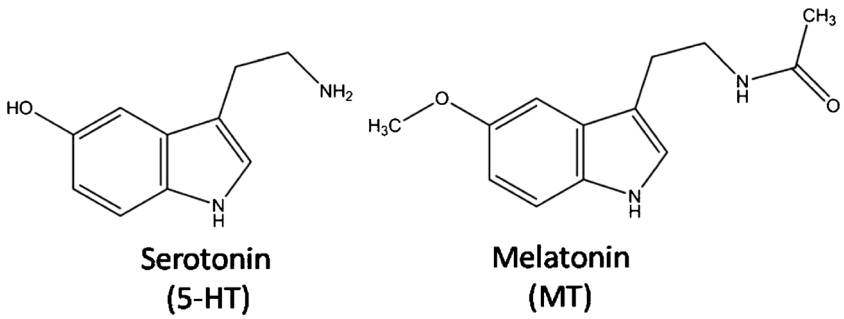

Fig. 1 Chemical structures of target analytes

planar CSPE consists of a conventional three-electrode configuration with a silver reference electrode, a carbon counter electrode and a 4 mm diameter carbon working electrode printed on a ceramic support.

The modified electrodes were prepared by casting 10 μL of a 0.50 mg mL^{-1} dispersion of each carbon nanomaterial (SWCNT, MWCNT, graphene oxide nanoribbons (GON) and graphene reduced nanoribbons (GRN)) on the CSPE.

Graphene nanoribbons detailed synthesis and characterization features have been previously reported [27]. In brief, graphene materials were synthesized from MWCNTs via the longitudinal unzipping method [28]. Using these GON (44 wt.% oxygen content), GRN (14 wt.% oxygen content) were obtained by chemical reduction with N_2H_4/NH_3 [29].

GON were dispersed to obtain a 0.50 mg mL^{-1} sample in water by ultra-sonication in a bath for 30 min. GRN were dispersed to obtain a 0.50 mg mL^{-1} dispersion in water/NH_3 (1 % v/v) by ultrasonication in a bath for 30 min, followed by tip sonication using a VCX130, (Sonics, Newtown, USA) for 2 min at 130 W.

SWCNTs were purchased from Sigma Chemical (St. Louis, MO, USA). SWCNT and MWCNTs were dispersed to obtain 0.50 mg mL^{-1} dispersion in dimethyl formamide (DMF) by ultrasonication in a bath for 30 min, followed by tip sonication using a VCX130, (Sonics, Newtown, USA) for 2 min at 130 W.

Sample preparation

Melatonin tablets and melatonin herb extract capsules were purchased at a local market. Extraction from tablets and capsules was carried out under dim light to prevent analyte degradation. The content of the capsules was diluted with 5 mL of MeOH, then vortexed during 30 s and sonicated in an ultrasound bath for 10 min. The resulting extract was filtered through a 0.20 μm syringe filter (Sartorius Ministart®) and stored in an amber vial. On the day of the experiment, solutions were prepared by diluting the stock solution with phosphate buffer 0.05 M.

Electrochemical procedure

The measurements were recorded using just 50 μL of the solution that permitted to cover the three electrodes. The electrochemical behavior of 5-HT and MT at the different electrodes in 50 mM phosphate buffer at pH 7.6 was examined using differential pulse voltammetry (DPV). DPV was performed with a potential range from −0.1 to +1.0 V, with 5 mV step potential, 25 mV pulse potential, 5 mVs^{-1} scan rate, 0.07 s pulse time and 3 s equilibration time.

In order to calculate the diffusion coefficient of MT, a study of cyclic voltammetry (CV) at different scan rates was displayed. CV was performed for 0.5 mM MT in 50 mM phosphate buffer at pH 7.6 in a bare CSPE using a potential range from −0.5 to +1.0 V with 5, 10, 25, 50, 100, 200 and 500 mV s^{-1} scan rates. Considering that for quasi-reversible systems such as MT, the plot of the peak intensity (i) versus the square root of the scan rate ($v^{1/2}$) is linear, the process follows the Randles-Sevcik diffusion model and the process is diffusion controlled. Consequently, the diffusion coefficient could be calculated for the electroactive molecule following Eq. 1, in which F is the Faraday constant, R is the gases constant, T is the temperature (298 K), n, is the number of transferred electrons (that is, 2) [23]; A, area of the electrodic surface (that is the geometric area of a CSPE, 0.0126 cm^2), D is the diffusion coefficient and c is the concentration of the electroactive specie.

$$i = 0.4463\left(\frac{F^3}{RT}\right)^{1/2} n^{3/2} A D^{1/2} c v^{1/2} \quad (1)$$

The effective electrochemical surface areas of the commercial and modified CSPE were estimated with the slope of the plot of Q vs. $t^{1/2}$ obtained by chronocoulometry using 0.5 mM MT in 50 mM phosphate buffer at pH 7.6. Taking into account the Eq. 2, described by Anson [30] the correspondent areas were calculated.

$$Q(t) = \frac{2nFAcD^{1/2}t^{1/2}}{\pi^{1/2}} + Q_{dl} + |Q_{ads} \quad (2)$$

In this equation, A is the effective electrochemical surface area of the working electrode (cm^2), c is the concentration of the electroactive species (mol/cm^3), n is the number of transfer electrons (that is, 2), F is the Faraday constant, and D is the diffusion coefficient of MT calculated above. Q_{dl} is the double layer charge, which could be eliminated by background subtraction, and Q_{ads} is the faradaic charge.

Results and discussion

Electrochemical detection of MT and 5-HT on carbon nanomaterial based electrodes

To explore the use of carbon nanomaterials on screen printed electrodes for electrochemical detection of 5-HT and MT, two sets of electrodes were studied: commercial based-carbon nanomaterials electrodes which are commercially available (SW-c, MW-c, GP-c where c indicates commercial) and modified ones (SW-m, MW-m, GON-m, GRN-m where m indicates modified) in which the carbon nanomaterial is used to modify the carbon ink-based electrodes (CSPE-c). Commercially available electrodes were used since they are a valuable analytical tool ready-to-use while modified ones were used as an alternative to allow a tailored in-lab electrode as required.

Table 1 Electrode terminology and estimated electroactive area of the carbon nanomaterial-based screen-printed electrodes

Commercial	Area (mm^2)	In-lab	Area (mm^2)
CSPE-c	0.95	SW-m	3.77
SW-c	2.46	MW-m	0.88
MW-c	1.23	GON-m	4.93
GP-c	3.16	GRN-m	9.70

Firstly, the effective electrochemical surface area was evaluated for the electrodes under study. Since the diffusion coefficient of MT has not been reported, it was calculated according to the Eq. 1 giving a value of 7.50×10^{-5} cm^2 s^{-1}. This value is in accordance with the diffusion coefficient for other electroactive molecules and permitted us to estimate the electroactive areas for the electrodes listed in Table 1.

For both electrode groups, SWCNTs based electrodes exhibited higher electroactive surfaces than MWCNTs and graphenes exhibited the highest ones. Interestingly, in-lab modified electrodes exhibited higher electroactive areas compared to those obtained for commercial ones, being graphene nanoribbon-based electrodes (GRN-m) the ones that showed the highest electroactive areas.

Secondly, the electrochemical behavior of 5-HT and MT was deeply explored by differential pulse voltammetry (DPV). Figure 2a shows the voltammograms obtained using the commercial electrodes. While CNT-based electrodes gave a good electrochemical response depicting two well-defined oxidation peaks for 5-HT and MT (highest sensitivity in SW-c and lowest oxidation potentials in MW-c), graphene-based ones exhibited a poor performance with non-defined voltammetric signals. In Fig. 2b is shown the voltammograms obtained for the target analytes using in-lab modified electrodes. GRN-m did not show a good electrochemical performance and non-well defined voltammograms for 5-HT and MT, while SW-m showed a good electrochemical behavior for 5-HT but not for MT. MW-m and GON-m depicted a well-defined voltammetric peaks for both molecules 5-HT and MT. Furthermore, GON-m showed not only the highest sensitivity but also a low oxidation potential for MT, exhibiting this electrode the best electroanalytical performance. Figure 2c shows a comparison between the best electrodes from each group. When SW-c were used, the oxidation peak currents for 5-HT and MT increased (1.8 times) while the oxidation peak potentials did not shift to a less positive oxidation values compared to bare CSPE. However, when GON-m were used, the oxidation peak current for 5-HT and MT increased significantly (2.4 times), and more importantly, a profound electro-catalysis was

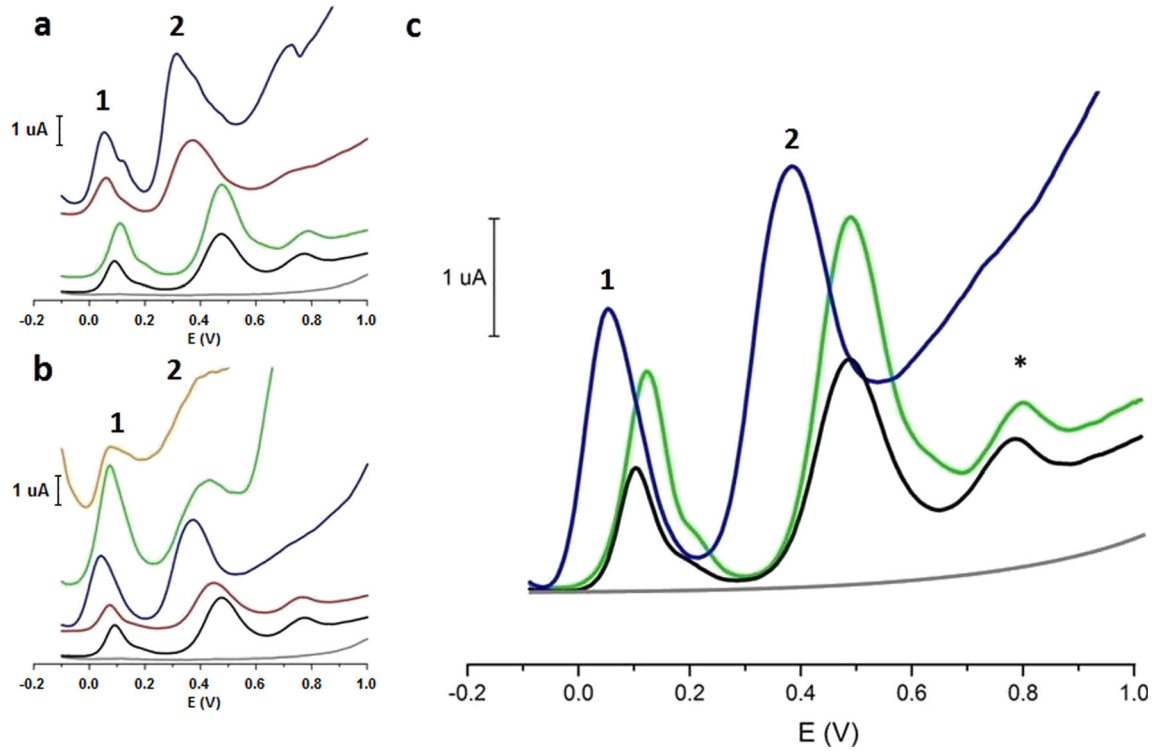

Fig. 2 Voltammograms for a mixture of 0.1 mM 5-HT (*peak 1*) and 0.5 mM MT (*peak 2*). **a** Commercial electrodes: bare CSPE (*black*), SW-c (*green*), MW-c (*red*) and GP-c (*blue*). **b** In-lab modified electrodes: bare CSPE (*black*), MW-m (*red*), GON-m (*blue*), SW-m (*green*) and GRN-m (*orange*). **c** Comparison between SW-c and GON-m. Bare CSPE used as control (*black*). Background signal in bare CSPE (*gray*). (*) corresponds to a second oxidation of MT. Reference electrode, Ag. Other Conditions: Phosphate buffer 50 mM pH 7.6, 5 mV step potential, 25 mV pulse potential, 5 mVs^{-1} scan rate, 0.07 s pulse time and 3 s equilibration time

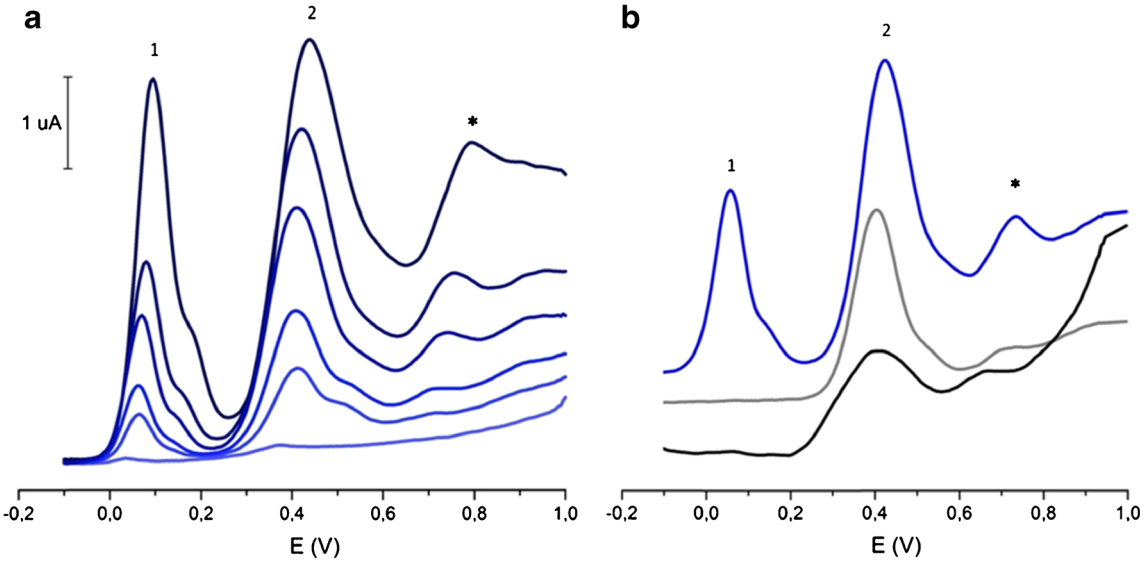

Fig. 3 **a** Voltammograms for simultaneous calibration of 5-HT (*peak 1*) and MT (*peak 2*). **b** Voltammograms for simultaneous determination of 5-HT (*peak 1*) and MT (*peak 2*) in capsule (*black*), tablet (*gray*) and spiked capsule with 0.1 mM 5-HT and 0.5 mM MT (*blue*). Note that (*) corresponds to a second oxidation potential for MT. Reference electrode, Ag. Other Conditions: phosphate buffer 50 mM pH 7.6, 5 mV step potential, 25 mV pulse potential, 5 mVs^{-1} scan rate, 0.07 s pulse time and 3 s equilibration time

noticed since the oxidation peak potentials shifted to a less positive oxidation values of +50 mV for 5-HT and +390 mV for MT compared to +110 mV for 5-HT and+450 mV for MT at a bare CSPE. They suppose an identical shift in ΔE=60 mV for both target molecules.

These results revealed that GON-m were the optimum electrodes to be used. They exhibited a profound electrocatalysis (decrease in the oxidation potentials in ΔE=60 mV), the highest sensitivity (enhancement in the amperometric currents), improved density current (26.25 $\mu A \cdot cm^{-2}$ and 36.33 $\mu A \cdot cm^{-2}$ in GON-m vs. 14.91 $\mu A \cdot cm^{-2}$ and 22.66 $\mu A \cdot cm^{-2}$ obtained on CSPE (geometric area= 0.12 cm^2) for 5-HT and MT, respectively) and, additionally, the lowest surface fouling because of their high electroactive area (resistance-to-fouling was increased in the order CSPE<SW-c<GON-m).

However, critically, this performance was not excellent enough (mainly for 5-HT detection, which fouled the electrode until 67 % after second measurement). As a consequence, disposability becomes the most rational approach to be investigated. To this end, for GON-m material, electrode modification reproducibility was also evaluated. An excellent inter-electrode reproducibility in the oxidation potentials (RSD ≤ 4.7 and ≤ 2.8 %, for 5-HT and MT, respectively) and in peak heights (RSD ≤ 5.9 and≤8.2 %, for 5-HT and MT, respectively) for n=7 electrodes was obtained. This excellent inter-electrode reproducibility indicates that these electrodes could be disposable, which constitute an extra advantage for this approach.

Analytical performance and sample analysis

The analytical performance was also evaluated using the in-lab modified GON-based electrodes. Well-defined voltammetric peaks at +50 mV for 5-HT and +390 mV for MT were obtained for each assayed concentration as depicted in Fig. 3a. As it is listed in Table 2, the resulting calibration plots were highly linear (R^2≥0.990) in the concentration range investigated for each analyte. Combination of the high sensitivity with a low noise level resulted in very good LODs (S/N=3).

The method was also applied to commercially available samples. As can be seen in Fig. 3b, the peak maximum of MT voltammograms of these samples assayed was obtained at +400 mV; this potential is highly coincident with the one obtained for the MT standard solution with a peak maximum at +390 mV. In addition, the two oxidation peaks for 5-HT and MT (at +50 mV for 5-HT and +400 mV for MT) were

Table 2 Analytical features of the method

Analyte	Regression equation[a]	R^2	Linear range (mM)	LOD (μM)	LOQ (μM)
MT	y=0.134+0.010x	0.991	0.005–3	1.1	3.8
5-HT	y=0.071+0.019x	0.996	0.001–2.5	0.4	1.1

[a] Regression equation is y=bx+a where y is the amperometric current (μA) and x is the analyte concentration (mM)

recorded in the spiked samples. Quantitatively, a very high agreement between the obtained values with those declared with quantitative and reproducible recoveries were obtained, as it is listed in Table 3. Quantitative and reproducible recoveries were obtained (94.4±0.2 and 102.8±0.6 % for MT and 5-HT, respectively) in the spiked capsule sample. Overall, these results indicated a very good accuracy of the method.

Although the analytical performance of the method for the chosen application was good, other potential interferents were also studied on GON-m electrodes. While the important neurotransmitter epinephrine did not show interference with an oxidation potential at higher values for those obtained for the target analytes (+1120 mV), the biogenic amines tyramine and tryptamine do interfere with an oxidation potential close to that of MT. However, the non-interference of epinephrine allowed the simultaneous detection of these three important neurotransmitters in other samples. Interestingly, uric acid was also assayed and it did not show a strong interference exhibiting an oxidation potential at +220 mV. It originated a partially resolved voltammogram peaks with a $\Delta E = \pm 20$ mV between 5-HT and MT becoming this approach also useful for the analysis of urine samples.

Finally, Table 4 lists the main analytical features obtained in the selected related works found in the literature involving the electrochemical sensing of MT and its precursors without separation techniques [20–24]. This work was the first approach using carbon nanomaterials and screen printed technology which had valuable advantages such as single use, disposability without losing performances. The LODs obtained were also competitive with the previous reported, taking advantage of the inherent miniaturization, which became a very important electrochemical screening approach. Additionally, the portability of the system makes it very valuable for wide spread use without the need of skilled personnel. All these features make these electrochemical approaches very valuable screening tools before the use of more sophisticated analytical techniques.

Conclusions

This work demonstrates that carbon nanomaterial (specifically graphene oxide nanoribbons)-based screen-printed electrodes, provide an easy, fast and reliable analytical tool for the simultaneous detection and determination of 5-HT and MT.

Table 3 Analysis of MT in commercial samples

Sample	MT declared (mg)	MT found (mg)[a]	Recovery (%)
Tablet	3.00	2.95±0.02	98.3±0.7
Capsule	1.80	1.76±0.05	97.8±2.8

[a] Values are expressed as mean value±SD

Table 4 Selected electro-analytical works for the simultaneous detection of 5-HT and MT

Analyte	Sample	Electrode	Technique	LOD	Remarks	Ref.
5-HT and dopamine	Human serum	GC ($PrNH_2$)	DPV	0.1 nM (5-HT) 0.1 nM (MT)	High electrocatalysis	[20]
5-HT; MT	Rabbit ileum	BDD	DPV	1.0 μM (5-HT) 2.2 μM (MT)	Real-time simultaneous detection of 5-HT and MT in vitro	[21]
MT	Commercial drugs	GC-MWs	CV	20 nM	High sensitivity	[22]
MT	Commercial drugs & urine	BDD	SWV	0.11 μM	Simplicity	[23]
MT	Commercial drugs	BDD	CV	0.01 mM	Low analysis time (2.5 min)	[24]
5-HT; MT	Commercial drugs	CNTs and graphene-based CSPE	DPV	0.4 μM (5-HT) 1.1 μM (MT)	Fast and simultaneous detection (120 s) Low sample consumption (50 μL) Disposability	This work

GC glassy carbon, *BDD* boron-doped diamond, *CV* cyclic voltammetry, *SWV* square-wave voltammetry

Screen-printed platforms modified with graphene oxide nanoribbons was clearly competitive in comparison with the other electrochemical approaches since it offered a very fast response time (120 s), low sample consumption (just 50 μL) and single use (disposability) because of their inherent miniaturization and excellent inter-electrode reproducibility. In addition, in comparison with others methodologies such as, HPLC or CE, the presented approach is a faster and simpler alternative, which avoids even the large use of toxic solvents.

Although the application given has been confined to the pharmaceutical analysis, the excellent performance obtained makes of this approach a promising one not only in the pharmaceutical quality control but in the determination of relevant neurotransmitters in urine and other related samples.

Acknowledgments The authors gratefully acknowledge financial support provided by the Spanish Ministry of Economy and Competitiveness (CTQ2011-28135) and from the NANOAVANSENS program from the Community of Madrid (S2013/MIT-3029). D. Federico Jose Vicente Gomez acknowledges BIP TII fellowship received from CONICET and D. Aída Martín acknowledges the FPU fellowship received from the Ministry of Education, Culture and Sports. The authors acknowledge to Dra. María Teresa Martínez and Dr. Javier Hernández-Ferrer from Instituto de Carboquímica ICB-CSIC of Zaragoza (Spain) for supplying GON and GRN samples.

References

1. Martín A, Escarpa A (2014) Graphene: the cutting-edge interaction between chemistry and electrochemistry. TrAC Trends Anal Chem 56:13–26
2. Martín A, López MÁ, González MC, Escarpa A (2015) Multidimensional carbon allotropes as electrochemical detectors in capillary and microchip electrophoresis. Electrophoresis 36:179
3. Pumera M, Escarpa A (2009) Nanomaterials as electrochemical detectors in microfluidics and CE: fundamentals, designs, and applications. Electrophoresis 30(19):3315–3323
4. Escarpa A (2012) Food electroanalysis: sense and simplicity. Chem Rec 12(1):72–91
5. Vitalini S, Gardana C, Zanzotto A, Fico G, Faoro F, Simonetti P, Iriti M (2011) From vineyard to glass: agrochemicals enhance the melatonin and total polyphenol contents and antiradical activity of red wines. J Pineal Res 51(3):278–285
6. Vitalini S, Gardana C, Simonetti P, Fico G, Iriti M (2013) Melatonin, melatonin isomers and stilbenes in Italian traditional grape products and their antiradical capacity. J Pineal Res 54(3):322–333
7. Gomez FJV, Raba J, Cerutti S, Silva MF (2012) Monitoring melatonin and its isomer in Vitis vinifera cv. Malbec by UHPLC-MS/MS from grape to bottle. J Pineal Res 52(3):349–355. doi:10.1111/j.1600-079X.2011.00949.x
8. Gomez FJV, Hernández IG, Martinez LD, Silva MF, Cerutti S (2013) Analytical tools for elucidating the biological role of melatonin in plants by LC-MS/MS. Electrophoresis 34(12):1749–1756
9. Kocadağli T, Yilmaz C, Gökmen V (2014) Determination of melatonin and its isomer in foods by liquid chromatography tandem mass spectrometry. Food Chem 153:151–156
10. Pothinuch P, Tongchitpakdee S (2011) Melatonin contents in mulberry (Morus spp.) leaves: effects of sample preparation, cultivar, leaf age and tea processing. Food Chem 128(2):415–419
11. Riga P, Medina S, García-Flores LA, Gil-Izquierdo Á (2014) Melatonin content of pepper and tomato fruits: effects of cultivar and solar radiation. Food Chem 156:347–352
12. Stürtz M, Cerezo AB, Cantos-Villar E, Garcia-Parrilla MC (2011) Determination of the melatonin content of different varieties of tomatoes (Lycopersicon esculentum) and strawberries (Fragaria ananassa). Food Chem 127(3):1329–1334
13. Karunanithi D, Radhakrishna A, Sivaraman KP, Biju VMN (2013) Quantitative determination of melatonin in milk by LC-MS/MS. J Food Sci Technol 51(4):805–812
14. Stehle JH, Saade A, Rawashdeh O, Ackermann K, Jilg A, Sebestény T, Maronde E (2011) A survey of molecular details in the human pineal gland in the light of phylogeny, structure, function and chronobiological diseases. J Pineal Res 51(1):17–43
15. Feldman JM, Lee EM (1985) Serotonin content of foods: effect on urinary excretion of 5-hydroxyindoleacetic acid. Am J Clin Nutr 42(4):639–643
16. Cao J, Murch SJ, O'Brien R, Saxena PK (2006) Rapid method for accurate analysis of melatonin, serotonin and auxin in plant samples using liquid chromatography-tandem mass spectrometry. J Chromatogr A 1134(1-2):333–337
17. Musijowski J, Pobozy E, Trojanowicz M (2006) On-line preconcentration techniques in determination of melatonin and its precursors/metabolites using micellar electrokinetic chromatography. J Chromatogr A 1104(1-2):337–345
18. Harumi T, Matsushima S (2000) Separation and assay methods for melatonin and its precursors. J Chromatogr B 747(1-2):95–110
19. Huang X, Mazza G (2011) Application of LC and LC-MS to the analysis of melatonin and serotonin in edible plants. Crit Rev Food Sci Nutr 51(4):269–284
20. Hasanzadeh M, Shadjou N, Omidinia E (2013) A novel electroanalytical method for simultaneous detection of two neurotransmitter dopamine and serotonin in human serum. J Neurosci Methods 219(1):52–60
21. Patel BA (2008) Continuous amperometric detection of co-released serotonin and melatonin from the mucosa in the ileum. Analyst 133(4):516–524
22. Qu W, Wang F, Hu S, Cui D (2005) Electrocatalytic properties and voltammetric determination of melatonin at a nanostructured film electrode. Microchim Acta 150(2):109–114
23. Levent A (2012) Electrochemical determination of melatonin hormone using a boron-doped diamond electrode. Diam Relat Mater 21:114–119
24. Ball AT, Patel BA (2012) Rapid voltammetric monitoring of melatonin in the presence of tablet excipients. Electrochim Acta 83:196–201
25. Yang X, Feng B, He X, Li F, Ding Y, Fei J (2013) Carbon nanomaterial based electrochemical sensors for biogenic amines. Microchim Acta 180(11-12):935–956. doi:10.1007/s00604-013-1015-6
26. Sanghavi BJ, Wolfbeis OS, Hirsch T, Swami NS (2015) Nanomaterial-based electrochemical sensing of neurological drugs and neurotransmitters. Microchim Acta 182:1–41. doi:10.1007/s00604-014-1308-4
27. Martin A, Hernandez-Ferrer J, Vazquez L, Martinez M-T, Escarpa A (2014) Controlled chemistry of tailored graphene nanoribbons for electrochemistry: a rational approach to optimizing molecule detection. RSC Adv 4(1):132–139. doi:10.1039/c3ra44235g
28. Kosynkin DV, Higginbotham AL, Sinitskii A, Lomeda JR, Dimiev A, Price BK, Tour JM (2009) Longitudinal unzipping of carbon nanotubes to form graphene nanoribbons. Nature 458(7240):872–876
29. Gao X, Jang J, Nagase S (2010) Hydrazine and thermal reduction of graphene oxide: reaction mechanisms, product structures, and reaction design. J Phys Chem C 114(2):832–842
30. Anson FC, Osteryoung RA (1983) Chronocoulometry: a convenient, rapid and reliable technique for detection and determination of adsorbed reactants. J Chem Educ 60(4):293–296